



LI-RADS v2017 categorisation of HCC using CT: Does moderate to severe fatty liver affect accuracy?

Seung Soo Kim¹ · Jeong Ah Hwang¹ · Hyeong Cheol Shin¹ · Seo-Youn Choi² · Tae Wook Kang³ · Sung Shick Jou¹ · Woong Hee Lee¹ · Suyeon Park⁴ · Nam Hun Heo⁵

Received: 16 March 2018 / Revised: 1 July 2018 / Accepted: 4 July 2018 / Published online: 2 August 2018
© European Society of Radiology 2018

Abstract

Objectives To compare the sensitivity of Liver Imaging Reporting and Data System (LI-RADS) v2017 for diagnosis of hepatocellular carcinoma (HCC) using multiphasic computed tomography (CT) between patients with and without moderate to severe fatty liver (MSFL).

Methods This retrospective study included a total of 106 high-risk patients with 112 pathologically proven HCCs who underwent multiphasic CT. Patients were classified as MSFL (24 men, 2 women; mean age, 59.5 years [range, 38–79 years]) and non-MSFL (64 men, 16 women; mean age, 62.9 years [range, 40–89 years]) groups according to unenhanced CT liver and spleen parenchymal attenuation. Two independent radiologists assigned LI-RADS categories and accessed HCC features on CT. Sensitivities for LR-5 assignment and frequencies of HCC features were compared between the two groups.

Results Sensitivities of LR-5 assignment for diagnosing HCCs were not significantly different between MSFL and non-MSFL groups (65.4% [17/26] vs. 76.7% [66/86] for reviewer 1, $p = 0.247$; 73.1% [19/26] vs. 76.74% [66/86] for reviewer 2, $p = 0.702$). No significant differences in the frequencies of arterial hyperenhancement, washout, and capsule were observed between the two groups (96.2% [25/26] vs. 98.8% [85/86], $p = 0.412$; 80.8% [21/26] vs. 89.5% [77/86], $p = 0.308$; and 53.8% [14/26] vs. 57% [49/86], $p = 0.778$, respectively).

Conclusions LI-RADS v2017 using CT showed comparable sensitivity for diagnosing HCC regardless of MSFL.

Key Points

- Using LI-RADS v2017 with CT, diagnosis of HCC in patients with MSFL showed similar sensitivity to that in patients without MSFL.
- Frequencies of major HCC features (arterial hyperenhancement, washout, and capsule) on CT between the MSFL and non-MSFL groups were not significantly different.
- LI-RADS using CT may be feasible for diagnosing HCC in patients with fatty liver.

Keywords Carcinoma, hepatocellular · Fatty liver · Multidetector computed tomography · Liver neoplasms

Abbreviations

CT	Computed tomography
HCC	Hepatocellular carcinoma
HU	Hounsfield units

ICC	Intraclass correlation coefficient
LC	Liver cirrhosis
LI-RADS	Liver Imaging Reporting and Data System
MSFL	Moderate to severe fatty liver

✉ Seung Soo Kim
radiology2008@hanmail.net

¹ Department of Radiology, Soonchunhyang University College of Medicine, Cheonan Hospital, Soonchunhyang6-gil, Dongnam-gu, Cheonan-si, Chungcheongnam-do 330-721, Republic of Korea

² Department of Radiology, Soonchunhyang University College of Medicine, Bucheon Hospital, Bucheon, Republic of Korea

³ Department of Radiology and Center for Imaging Science, Samsung Medical Center, Sungkyunkwan University School of Medicine, Seoul, Republic of Korea

⁴ Department of Biomedical Statistics, Soonchunhyang University Seoul Hospital, Seoul, Republic of Korea

⁵ Clinical Trial Center, Soonchunhyang University Cheonan Hospital, Cheonan-si, Chungcheongnam-do, Republic of Korea

NAFLD	Non-alcoholic fatty liver disease
ROI	Region of interest
TIV	Tumour in vein

Introduction

Hepatocellular carcinoma (HCC) is the most common malignant hepatic neoplasm associated with chronic liver disease [1]. Common causes of liver cirrhosis (LC) are chronic viral B or C hepatitis and alcohol abuse, and these conditions are often accompanied by fatty changes of the liver [2, 3]. In addition, non-alcoholic fatty liver disease (NAFLD) is also considered a cause of chronic liver disease [3, 4]. Therefore, a portion of HCCs develop in the setting of fatty liver. When there is fatty change in the liver, liver attenuation decreases on computed tomography (CT) [5, 6].

According to current guidelines provided by the American Association for the Study of Liver Disease and European Association for the Study of the Liver, HCCs can be diagnosed based on imaging findings without histopathologic confirmation [7, 8]. Recently, the Liver Imaging Reporting and Data System (LI-RADS) was developed to reduce interobserver variability in lesion interpretation and to improve communication with referring clinicians [9, 10]. In LI-RADS, diagnosis of HCC is based mainly on lesion size, threshold growth, and the three major imaging findings of arterial hyperenhancement, washout, and capsule [9–11]. Among the major imaging findings of HCC, washout is defined as visually assessed reduction in enhancement relative to background liver on portal venous and/or delayed phase [10–13]. However, with moderate to severe fatty liver (MSFL), it may be difficult to evaluate washout on CT because of reduced attenuation of the surrounding hepatic parenchyma. In addition, some HCCs in patients with MSFL already show higher attenuation than the surrounding liver parenchyma on unenhanced images, which may affect the appearance of washout and capsule.

The diagnostic performance of LI-RADS has been investigated by several research groups [14–17], but to the best of our knowledge, no study has evaluated if there is a difference in categorisation of HCC using CT between patients with and without MSFL. Therefore, the purpose of our study was to compare the sensitivity of LI-RADS v2017 for diagnosis of HCC using multiphasic CT between patients with and without MSFL.

Materials and methods

Our institutional review board approved this retrospective study, and the need for informed consent was waived for all patients.

Study population

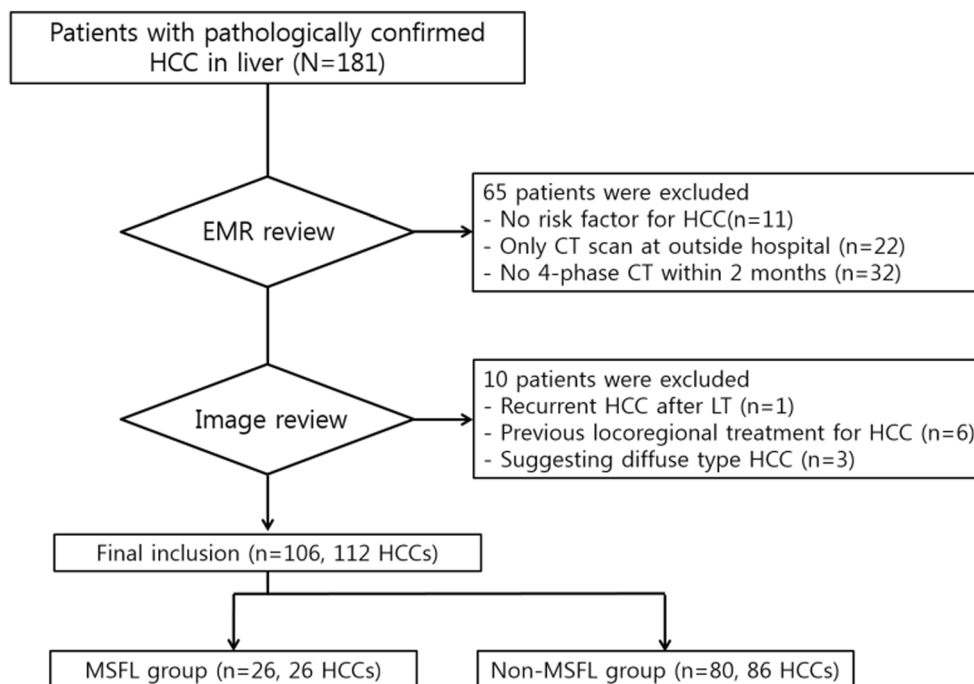
Medical records of patients who were admitted to our institution from January 2006 through December 2016 were reviewed. This resulted in identification of 181 patients with histopathologically confirmed HCC by percutaneous biopsy or surgical resection of the liver. For percutaneous biopsy, the investigator obtained at least two biopsy specimens using an 18-gauge core needle under ultrasonography guidance. One or two pathologists diagnosed HCC by consensus, and there were no indeterminate histopathologic results for the diagnosis of HCC in the 181 patients identified. After reviewing electronic medical records, 116 patients were enrolled based on the following inclusion criteria: (1) patients at high risk for HCC according to LI-RADS v2017 [10]; adult (older than 18 years) patients with LC, chronic hepatitis B, and current or prior HCC with or without cirrhosis and (2) patients who performed 4-phase CT at our institute within 2 months before and after pathologic diagnosis of HCC. Thereafter, one abdominal radiologist (S.S.K. with 10 years of experience) who was not blinded to the medical records and histopathologic findings reviewed the CT images. Ten patients were excluded on the basis of image review using the following criteria: (1) patient with recurrent HCC after liver transplantation ($n = 1$); (2) patients with previous history of locoregional treatment for HCC ($n = 6$); and (3) patients who had only diffuse type HCC, which might be problematic in the setting of steatosis ($n = 3$). Finally, 106 patients with 112 pathologically proven HCCs were included in this study. In patients with multiple HCCs, only pathologically proven lesions were enrolled.

The radiologist also measured Hounsfield units (HU) of the spleen and liver parenchyma adjacent to the HCC for enrolled patients. A region of interest (ROI) was drawn on the unenhanced image for unaffected hepatic parenchyma of the same segment and same level as well as the spleen. Measurements of ROI were taken three times and averaged, and the average value was used for evaluation. MSFL was defined as follows: (1) unenhanced CT liver parenchymal attenuation < 48 HU or (2) unenhanced CT liver attenuation minus spleen attenuation < -2 [18]. As a result, 26 patients with 26 HCCs were included in the MSFL group, and the remaining 80 patients with 86 HCCs formed the non-MSFL group. A detailed flow diagram describing patient selection is shown in Fig. 1.

CT imaging technique

All CT scans were performed using one of the following multidetector row scanners at our institution: Light Speed Ultra ($n = 26$), Light Speed VCT ($n = 52$), Discovery CT750 ($n = 13$), and Optima CT660 ($n = 11$) (all GE Healthcare), and Brilliance iCT 256 ($n = 4$) (Philips Healthcare). Each patient

Fig. 1 Inclusion flow chart for the study population



received 120–140 mL of non-ionic contrast material (Iomeron 350, Bracco; Omnipaque 350, GE Healthcare; Bonorex 350, Central Medical Service; or Xenetix 350, Guerbet) through an 18-gauge angiographic catheter inserted into an antecubital vein at a rate of 3.0–4.0 mL/sec using an automated injection device. All CT examinations included unenhanced and contrast-enhanced imaging through the liver with hepatic arterial, portal venous, and delayed phases. Hepatic arterial phase imaging automatically began 10–15 seconds after the trigger attenuation threshold (100 HU) was reached at the level of the supraceliac abdominal aorta. Portal venous and delayed phases were obtained with delays of 60–70 and 180 s, respectively, after the start of contrast material administration. CT examinations were performed with the following parameters: tube voltage, 120 kVp; detector collimation, 0.625 to 1.250 mm; table pitch, 1:0.984 to 1.375; matrix, 512 x 512; and reconstruction intervals, 5.00 mm.

Image analysis

Two abdominal radiologists (H.C.S. and J.A.H., with 23 and 8 years of experience, respectively) evaluated CT images. Although they were aware that the enrolled population comprised high-risk patients and that this study attempted to assess LI-RADS categorisation of hepatic tumours, they were blinded to the objective of study and all clinical results. Both reviewers categorised hepatic tumours using LI-RADS on a picture archiving and communication system (DEJA-VIEW, Dongeun Information Technology). Prior to image review, each reader was provided a 1-hour lecture and hands-on

instruction detailing LI-RADS v2017 using information provided on the ACR website (<http://www.acr.org>). They independently reviewed the datasets and recorded six imaging features for each lesion: (1) tumour size, (2) presence of arterial hyperenhancement, (3) presence of washout, (4) presence of capsule, (5) attenuation on the unenhanced image, and (6) presence of tumour in vein (TIV). Tumour size (mm) was measured as the longest diameter of the lesion on axial portal venous or delayed phase images in which the tumour margin was most sharply demarcated. Arterial hyperenhancement was defined as non-rim-like enhancement in arterial phase unequivocally greater in whole or in part than the liver. Washout was defined as nonperipheral visually assessed temporal reduction in enhancement in whole or in part relative to composite liver tissue from earlier to later phase resulting in hypoenhancement in the portal venous and/or delayed phase. Capsule was defined as smooth peripheral rim enhancement during the portal venous and/or delayed phase. Attenuation on the unenhanced image was considered to be hyperattenuation, when attenuation of a lesion was higher than that of unaffected liver, isoattenuation, when it was similar to that of the unaffected liver, and hypoattenuation, when it was lower than that of the unaffected liver. If a lesion was partially hypo- or hyperattenuating, it was categorised based on the predominant attenuation. In LI-RADS v2017, category LR-5v is replaced with LR-TIV, which is defined as unequivocal enhancing soft-tissue TIV regardless of visualisation of a parenchymal mass [10]. Reviewers then assigned LI-RADS categories (LR-TIV: tumour in vein, LR-1: definitely benign, LR-2: probably benign, LR-3: indeterminate probability of malignancy, LR-4: probably HCC, LR-5: definitely HCC,

Table 1 Demographics of enrolled patients and HCCs

Variable	MSFL	non-MSFL	<i>p</i> value
By patient	<i>N</i> = 26	<i>N</i> = 80	
Age (years)‡	59.5 ± 13 (38–79)	62.9 ± 10.6 (40–89)	0.920
Sex			0.229
Male	24 (92.3%)	64 (80%)	
Female	2 (7.7%)	16 (20%)	
Child-Pugh class			0.008
A	17 (65.4%)	68 (85%)	
B	6 (23.1%)	12 (15%)	
C	3 (11.5%)	0 (0%)	
Cause of liver disease			0.039
Hepatitis B	8 (30.8%)	42 (52.5%)	
Hepatitis C	3 (11.5%)	8 (10%)	
Alcoholism	9 (34.6%)	21 (26.25%)	
Others	6 (23.1%)	9 (11.25%)	
By lesion	<i>N</i> = 26	<i>N</i> = 86	
Pathologic confirmation			0.01§
Percutaneous biopsy	7 (26.9%)	48 (55.8%)	
Surgical resection	19 (73.1%)	38 (44.2%)	

Note: Unless otherwise indicated, data are numbers, with percentages in parentheses

‡ Data are mean ± standard deviation, with range in parentheses

HCC hepatocellular carcinoma, MSFL moderate to severe fatty liver

§ *p* value by chi-square test

and LR-M: probably or definitely malignant, not specific for HCC) [10]. A third reader (S-Y.C. with 9 years of experience) resolved any discrepancies on CT findings and measured tumour size in the same way.

Statistical analysis

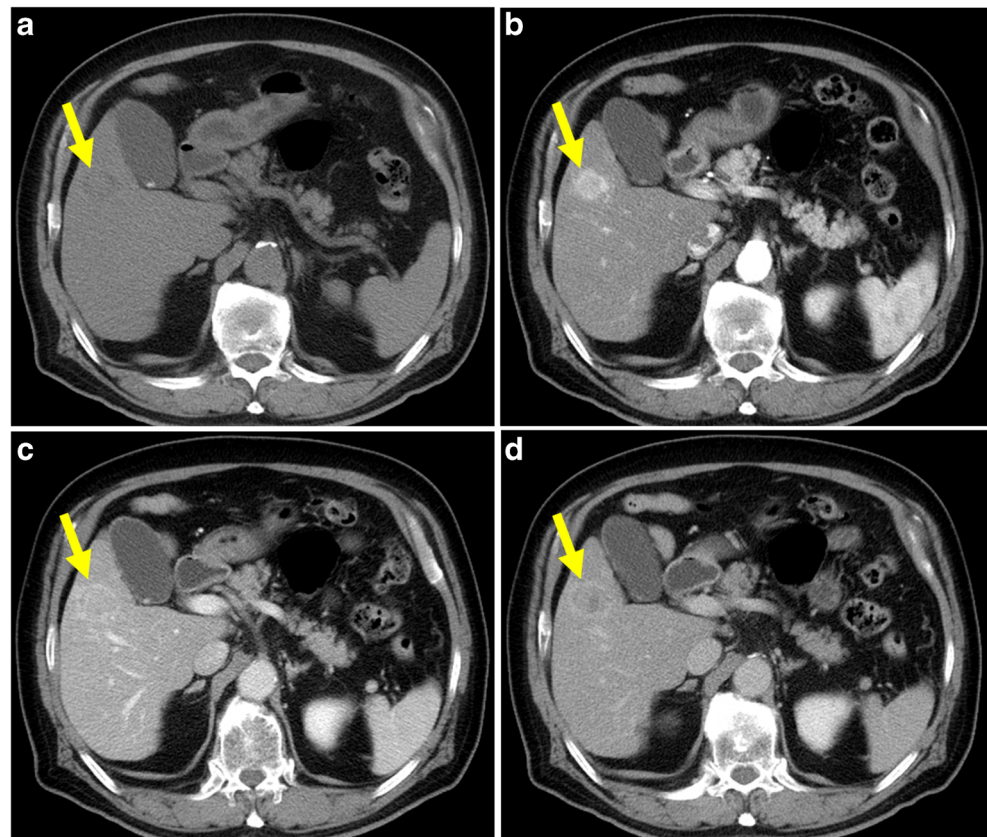
Comparison between the two groups was assessed by t-test for continuous variables and by Fischer's exact or chi-square test for categorical variables. The LI-RADS categorisations of HCCs between the two groups for each reviewer were compared using Fisher's exact test. Chi-square or Fisher's exact test were used to compare the frequencies of each HCC feature by consensus review between MSFL and non-MSFL groups. Discrepancies between the two radiologists regarding LR-5 assignment, CT findings, and LI-RADS scoring results of HCCs were used to assess interobserver agreement with the following scales: poor, 0.00–0.20; fair, 0.21–0.40; moderate, 0.41–0.60; substantial, 0.61–0.80; and excellent, 0.81–1.00. Interobserver agreement in LR-5 assignments and HCC imaging features between the two radiologists was evaluated by measuring the kappa value. Interobserver agreement in tumour size was assessed by calculating the intraclass correlation coefficient (ICC). Finally, the LI-RADS scoring results

for HCCs of each of the two reviewers were compared using Cohen's kappa coefficient. A two-sided *p* value less than 0.05 was considered to indicate statistical significance. All statistical analyses were performed using PASW statistical software (version 14.0, SPSS Inc.) and R 3.1.2 (<http://www.R-project.org/>).

Results

The clinical characteristics of enrolled patients and HCCs are summarised in Table 1. Patients in the MSFL group showed lower prevalence of Child-Pugh class A and hepatitis B than the non-MSFL group (65.4% [17/26] vs. 85% [68/80], *p* = 0.008 and 30.8% [8/26] vs. 52.5% [42/80], *p* = 0.039, respectively). There was no significant difference in age or sex between groups. HCCs in the MSFL group were more frequently confirmed by surgical resection relative to non-MSFL group (73.1% [19/26] vs. 44.2% [38/80], *p* = 0.01). The mean unenhanced CT liver parenchymal attenuation and mean unenhanced CT liver attenuation minus spleen attenuation in the MSFL group were 42.5 ± 6.8 HU (range, 24 to 53.8 HU) and -6.5 ± 5.1 (range, -21.5 to -0.3), respectively, and those in the non-MSFL group were 58.4 ± 5.9 HU (range, 49.1 to 77.3 HU) and 10.1 ± 10.4 (range, 0.4 to 74.7).

Fig. 2 Surgically proven hepatocellular carcinoma in a 74-year-old male patient with moderate to severe fatty liver. **(a)** Axial unenhanced CT image shows a 27-mm hypoattenuating mass in segment V of the liver. Unenhanced CT liver parenchymal attenuation and unenhanced CT liver attenuation minus spleen attenuation were 41.5 HU and -3.5, respectively. **(b)** Axial arterial phase contrast-enhanced CT image shows hyperenhancement of the mass. **(c, d)** Axial portal venous and delayed phase contrast-enhanced CT images show washout and capsule of the mass. Both reviewers scored this observation as LR-5



LI-RADS categorisation of HCCs

Sensitivity of LR-5 assignment was not significantly different between the MSFL and non-MSFL groups (65.4% [17/26] vs. 76.7% [66/86] for reviewer 1, $p = 0.247$; 73.1% [19/26] vs. 76.74% [66/86] for reviewer 2, $p = 0.702$), and there were no significant differences in other LI-RADS categorisations of HCCs between the two groups (Fig. 2). Details of the LI-RADS categories of HCCs are provided in Table 2. Interobserver agreement was substantial-to-excellent for assigning LR-5 ($k = 0.674$ – 0.821).

Imaging features of HCCs

Tumour sizes as assessed by a third reviewer were not significantly different between the MSFL and non-MSFL groups (37.7 ± 24.3 mm; range, 12–110 mm vs. 54.5 ± 44.7 mm; range, 8–189 mm, respectively, $p = 0.200$). A total of six (23.1%) and 14 (16.3%) HCCs in the MSFL and non-MSFL groups were smaller than 20 mm, respectively ($p = 0.559$). Using a consensus method, the frequencies of all three major imaging features (arterial hyperenhancement, washout, and capsule) were not significantly different between MSFL and

Table 2 LI-RADS categorisation of HCCs

	Reviewer 1			Reviewer 2		
	MSFL ($n = 26$)	non-MSFL ($n = 86$)	p value [‡]	MSFL ($n = 26$)	non-MSFL ($n = 86$)	p value [‡]
LR-5	17 (65.4%)	66 (76.7%)	0.247	19 (73.1%)	66 (76.74%)	0.702
LR-4	5 (19.2%)	5 (5.8%)	0.050	3 (11.5%)	6 (6.98%)	0.431
LR-3	2 (7.7%)	8 (9.3%)	1.000	2 (7.7%)	4 (4.65%)	0.622
LR-TIV	2 (7.7%)	6 (7%)	1.000	2 (7.7%)	9 (10.47%)	1.000
LR-M	0 (0%)	1 (1.2%)	1.000	0 (0%)	1 (1.16%)	1.000

Note: Data are numbers of HCCs, with percentages in parentheses

LI-RADS Liver Imaging Reporting and Data System, HCC hepatocellular carcinoma, MSFL moderate to severe fatty liver

‡ Categorisation of HCCs were compared using Fisher's exact test

non-MSFL groups (96.2% [25/26] vs. 98.8% [85/86], $p = 0.412$; 80.8% [21/26] vs. 89.5% [77/86], $p = 0.308$; and 53.8% [14/26] vs. 57% [49/86], $p = 0.778$, respectively). In subgroup analysis according to tumour size, there were no statistically significant differences in arterial hyperenhancement, washout, and capsule between the two groups (Table 3). Two HCCs (7.7%) in the MSFL group showed higher attenuation than background liver on unenhanced images without evidence of haemorrhage, and all of HCCs in the non-MSFL group revealed iso to low attenuation ($p = 0.052$). One of the two HCCs that were hyperattenuating on the unenhanced image did not show washout (Fig. 3).

Interobserver agreement

Interobserver agreement for overall imaging features including arterial hyperenhancement, washout, capsule, and attenuation on the unenhanced image was moderate ($k = 0.440$ – 0.492). The kappa value regarding washout was 0.537 in the MSFL group and 0.284 in the non-MSFL group, indicating moderate and fair agreement, respectively. Capsule agreement was moderate in the MSFL group ($k = 0.442$) and substantial

in the non-MSFL group ($k = 0.611$). For all patients, interobserver agreements for washout and capsule were moderate ($k = 0.447$ and 0.481 , respectively). Interobserver agreements were almost perfect for measured tumour size in both groups (ICC = 0.997 and 0.998, respectively) (Table 4). The distribution of LI-RADS scoring results for HCCs obtained by the two reviewers is shown in Table 5. The overall interobserver agreement (k score) for LR scores between reviewers 1 and 2 was 0.659 (confidence interval: 0.514–0.803), indicating substantial agreement.

Discussion

Despite differences in unenhanced liver parenchymal attenuation, the present study showed that LI-RADS using CT had comparable sensitivity for LR-5 assignment of HCCs in patients with and without MSFL and that there were no significant differences in major imaging findings of HCCs between MSFL and non-MSFL groups.

Regarding HCC in conditions with fatty liver, a previous study [19] reported that 100% and 70% of HCCs in patients with NAFLD showed arterial hyperenhancement and washout on CT. However, that study only included six (28.6%) patients with MSFL and did not compare CT findings of HCCs between patients with and without fatty liver. In our study, there were no significant differences in sensitivities for diagnosis of HCC using LI-RADS between patients with and without MSFL, although sensitivities in the MSFL group were slightly lower than those in the non-MSFL group (65.4% vs. 76.7% for reviewer 1, $p = 0.247$; 73.1% vs. 76.74% for reviewer 2, $p = 0.702$). The sensitivities of our study were slightly higher than those of previous reports [14, 15, 20]; this can be explained by the principle of LI-RADS according to tumour size [10]. Among the enrolled HCCs, 20 (76.9%) in the MSFL group and 72 (83.7%) in the non-MSFL group were equal to or larger than 20 mm, in contrast, there were only four HCCs smaller than 10 mm. Moreover, almost all HCCs (98.2%) showed arterial hyperenhancement, and were therefore frequently categorised as LR-5.

It is not surprising that arterial hyperenhancement of HCCs between MSFL and non-MSFL groups was not significantly different (96.2% vs. 98.8%, $p = 0.412$), because reduced attenuation of the surrounding hepatic parenchyma would not interfere with the evaluation of arterial hyperenhancement. We attributed the presence of arterial hyperenhancement in almost all HCCs to the large size of the enrolled HCCs. The results of our study are concordant with those of Joo et al [14], who demonstrated that 91.6% (141/154) of HCCs equal to or larger than 20 mm showed arterial hyperenhancement on CT.

Before conducting the current investigation, we hypothesised that washout would be masked in the MSFL group by low attenuation of the liver parenchyma. However, washout

Table 3 Comparison of frequencies of HCC imaging features between MSFL and non-MSFL groups

Variable	MSFL ($n = 26$)	non-MSFL ($n = 86$)	p value
Tumour size (mm)‡	37.7 ± 24.3 (12–110)	54.5 ± 44.7 (8–189)	0.200
< 20 mm	23.1 (6/26)	16.3 (14/86)	0.559
≥ 20 mm	76.9 (20/26)	83.7 (72/86)	
Arterial hyperenhancement			
All tumour sizes	96.2 (25/26)	98.8 (85/86)	0.412
< 20 mm	83.3 (5/6)	92.9 (13/14)	0.521
≥ 20 mm	100 (20/20)	100 (72/72)	N/A
Washout			
All tumour sizes	80.8 (21/26)	89.5 (77/86)	0.308
< 20 mm	83.3 (5/6)	78.8 (11/14)	1.000
≥ 20 mm	80 (16/20)	91.7 (66/72)	0.216
Capsule			
All tumour sizes	53.8 (14/26)	57 (49/86)	0.778§
< 20 mm	16.7 (1/6)	42.9 (6/14)	0.354
≥ 20 mm	65 (13/20)	59.7 (43/72)	0.798
Attenuation on unenhanced image			0.052
High	7.7 (2/26)	0 (0/86)	
Iso to low	92.3 (24/26)	100 (86/86)	

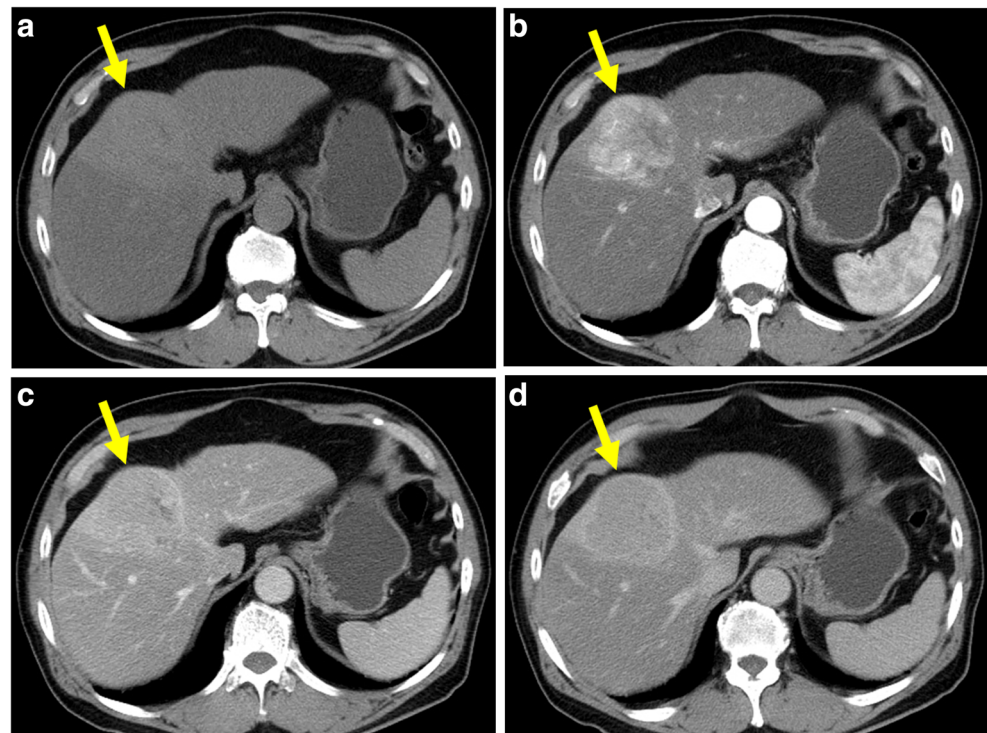
Note: Unless otherwise indicated, data are percentages (numbers used for calculation)

‡ Data are mean ± standard deviation, with range in parentheses

HCC hepatocellular carcinoma, MSFL moderate to severe fatty liver

§ p value by chi-square test

Fig. 3 Surgically proven hepatocellular carcinoma in a 72-year-old male patient with moderate to severe fatty liver. (a) Axial unenhanced CT image shows a 74-mm hyperattenuating mass in segment IV of the liver. Unenhanced CT liver parenchymal attenuation and unenhanced CT liver attenuation minus spleen attenuation were 24 HU and -7.9, respectively. (b) Axial arterial phase contrast-enhanced CT image shows hyperenhancement of the mass. (c, d) Axial portal venous and delayed phase contrast-enhanced CT images show the capsule. Although the mass was recorded as having no washout, this observation was assigned as LR-5 regardless of the presence of washout.



appearance was not significantly different between MSFL and non-MSFL groups (80.8% vs. 89.5%, $p = 0.308$), even in HCCs smaller than 20 mm (83.3% vs. 78.8%, $p = 1.000$). Although the exact mechanism of washout in HCC has not been elucidated, several factors are thought to influence this imaging finding. First, the number of neovascularised arteries may be greater in HCC than in surrounding liver parenchyma, which can lead to early venous drainage via neovascularisation. Second, surrounding fibrotic parenchyma retains contrast media. Third, HCCs do not receive portal flow. In contrast, liver parenchyma has a portal venous supply. Fourth, HCCs have decreased extracellular volume because of high tumoural cellularity, which reduces filling with contrast media [21]. These complex mechanisms may explain why the decrease in liver attenuation did not affect the appearance of washout.

The frequency of capsule was not significantly different between MSFL and non-MSFL groups (53.8% vs. 57%, $p = 0.778$). Capsule is attributed to slow flow within intracapsular vessels and contrast media retention within the extravascular space of the capsule, therefore surrounding fatty liver parenchyma may not prevent the capsule from appearing [10, 12, 22]. Capsule was observed at a lower frequency than arterial hyperenhancement and washout in both groups (96.2% vs. 98.8% and 80.8% vs. 89.5%, respectively), consistent with the results of previous studies [14, 23].

Iannaccone et al [19] reported that four (20%) HCCs in patients with fatty liver revealed higher attenuation than the surrounding liver on unenhanced images. In the present study, two (7.7%) HCCs in the MSFL group showed similar imaging features. Although one of the two hyperattenuating HCCs on

Table 4 Interobserver agreement for assigning LR-5 and imaging features of HCCs

	MSFL ($n = 26$)	Non-MSFL ($n = 86$)	All ($n=112$)
LR-5 assignment	0.821 (0.586–1.056)	0.674 (0.488–0.861)	0.714 (0.564–0.865)
Tumour size	0.997 (0.995–0.998)	0.998 (0.996–0.999)	0.997 (0.996–0.998)
Overall imaging features	0.440 (0.266–0.614)	0.492 (0.238–0.746)	0.455 (0.310–0.599)
Arterial hyperenhancement	N/A	N/A	N/A
Washout	0.537 (0.214–0.860)	0.284 (0.000–0.687)	0.447 (0.192–0.703)
Capsule	0.442 (0.252–0.961)	0.611 (0.305–0.916)	0.481 (0.319–0.644)
Attenuation on unenhanced image	N/A	0.649 (0.016–1.281)	0.663 (0.043–1.000)

Note: Data are kappa values, except for tumour size, which are intraclass correlation coefficients

Data in parentheses are 95% confidence intervals

HCC hepatocellular carcinoma, MSFL moderate to severe fatty liver

Table 5 Comparison of LI-RADS scoring results for HCCs obtained by reviewers 1 and 2

Reviewer 1	Reviewer 2					Total
	LR-5	LR-4	LR-3	LR-TIV	LR-M	
LR-5	78 (69.64%)	1 (0.89%)	0 (0.0%)	4 (3.57%)	0 (0.0%)	83 (74.11%)
LR-4	4 (3.57%)	5 (4.46%)	1 (0.89%)	0 (0.0%)	0 (0.0%)	10 (8.93%)
LR-3	2 (1.79%)	3 (2.68%)	5 (4.46%)	0 (0.0%)	0 (0.0%)	10 (8.93%)
LR-TIV	1 (0.89%)	0 (0.0%)	0 (0.0%)	7 (6.25%)	0 (0.0%)	8 (7.14%)
LR-M	0 (0.0%)	0 (0.0%)	0 (0.0%)	0 (0.0%)	1 (0.89%)	1 (0.89%)
Total	85 (75.89%)	9 (8.04%)	6 (5.36%)	11 (9.82%)	1 (0.89%)	112 (100.0%)

Note: Data are numbers of HCCs, with percentages in parentheses

LI-RADS Liver Imaging Reporting and Data System, HCC hepatocellular carcinoma

unenanced images was evaluated as having no washout, it was categorised as LR-5 because of the presence of arterial hyperenhancement and capsule. Further studies with a larger population are warranted to evaluate the impact of HCC attenuation on unenhanced image for assessment of washout and capsule.

Interobserver agreement between two reviewers for categorisation of HCCs, including LR-5, was substantial. Moderate interobserver agreements were observed for assessment of washout, capsule, and overall imaging features. Almost perfect agreement was obtained for measurement of tumour size. These results are similar to those of previous reports [14, 15, 20, 23].

Our study had several limitations. First, the retrospective design of the present study for determining sensitivity using a pathologically proven pool of patients could have introduced selection and verification biases. Therefore, the sensitivity of LI-RADS measured in this study is not generalizable. Second, there were fewer HCCs in the MSFL group ($n = 26$) than in the non-MSFL group ($n = 86$) and were small number of enrolled HCCs smaller than 20 mm (17.9% [20/112]). Third, MSFL was not histopathologically confirmed, and there was some overlap in unenhanced CT liver parenchymal attenuation between the two groups. Fourth, we did not include other hepatic lesions such as hemangiomas or cholangiocarcinomas. Further studies are needed to assess the specificity of LI-RADS in patients with MSFL. Fifth, although most patients underwent magnetic resonance imaging or CT follow-up after pathologic confirmation, there might be some HCCs missed.

In conclusion, LI-RADS v2017 using CT showed comparable sensitivity for diagnosis of HCCs in patients with MSFL and those without. Frequencies of major HCC features were not significantly different between patients with and without MSFL. Our data suggest that LI-RADS using CT is feasible option for diagnosing HCC in patients with fatty liver.

Funding This research did not receive any specific grant from funding agencies in the public, commercial or not-for-profit sectors.

This work was supported by the Soonchunhyang University Research Fund.

Compliance with ethical standards

Guarantor The specific guarantor of this publication is Sung Shick Jou, the head of the Radiology Department of Soonchunhyang University College of Medicine, Cheonan Hospital, Republic of Korea

Conflict of interest The authors of this manuscript declare no relationships with any companies, whose products or services may be related to the subject matter of the article.

Statistics and biometry Suyeon Park and Nam Hun Heo kindly provided statistical advice for this manuscript.

Informed consent Written informed consent was waived by the Institutional Review Board because of the retrospective nature of the study.

Ethical approval Institutional Review Board approval was obtained.

Methodology Retrospective, observational, performed at one institution

References

1. Bruix J, Sherman M (2005) Management of hepatocellular carcinoma. *Hepatology* 42:1208–1236
2. Schafer DF, Sorrell MF (1999) Hepatocellular carcinoma. *Lancet* 353:1253–1257
3. Younossi ZM, Stepanova M, Afendy M et al (2011) Changes in the prevalence of the most common causes of chronic liver diseases in the United States from 1988 to 2008. *Clin Gastroenterol Hepatol* 9: 524–530. e521
4. Angulo P (2002) Nonalcoholic fatty liver disease. *N Engl J Med* 346:1221–1231
5. Baffy G, Brunt EM, Caldwell SH (2012) Hepatocellular carcinoma in non-alcoholic fatty liver disease: an emerging menace. *J Hepatol* 56:1384–1391
6. Boyce CJ, Pickhardt PJ, Kim DH et al (2010) Hepatic steatosis (fatty liver disease) in asymptomatic adults identified by unenhanced low-dose CT. *AJR Am J Roentgenol* 194:623–628
7. Bruix J, Sherman M (2011) Management of hepatocellular carcinoma: an update. *Hepatology* 53:1020–1022

8. European Association For The Study Of The Liver (2012) EASL–EORTC clinical practice guidelines: management of hepatocellular carcinoma. *J Hepatol* 56:908–943
9. Mitchell DG, Bruix J, Sherman M, Sirlin CB (2015) LI-RADS (Liver Imaging Reporting and Data System): Summary, discussion, and consensus of the LI-RADS Management Working Group and future directions. *Hepatology* 61:1056–1065
10. Elsayes KM, Hooker JC, Agrons MM et al (2017) 2017 Version of LI-RADS for CT and MR Imaging: An Update. *Radiographics* 37: 1994–2017
11. Tang A, Bashir MR, Corwin MT et al (2017) Evidence Supporting LI-RADS Major Features for CT-and MR Imaging–based Diagnosis of Hepatocellular Carcinoma: A Systematic Review. *Radiology* 286:29–48
12. Choi JY, Lee JM, Sirlin CB (2014) CT and MR imaging diagnosis and staging of hepatocellular carcinoma: part II. Extracellular agents, hepatobiliary agents, and ancillary imaging features. *Radiology* 273:30–50
13. Yoon JH, Park JW, Lee JM (2016) Noninvasive diagnosis of hepatocellular carcinoma: elaboration on Korean Liver Cancer Study Group-National Cancer Center Korea practice guidelines compared with other guidelines and remaining issues. *Korean J Radiol* 17:7–24
14. Joo I, Lee JM, Lee DH, Ahn SJ, Lee ES, Han JK (2017) Liver imaging reporting and data system v2014 categorisation of hepatocellular carcinoma on gadoteric acid-enhanced MRI: Comparison with multiphasic multidetector computed tomography. *J Magn Reson Imaging* 45:731–740
15. Zhang YD, Zhu FP, Xu X et al (2016) Classifying CT/MR findings in patients with suspicion of hepatocellular carcinoma: Comparison of liver imaging reporting and data system and criteria-free Likert scale reporting models. *J Magn Reson Imaging* 43:373–383
16. Ehman EC, Behr SC, Umetsu SE et al (2016) Rate of observation and inter-observer agreement for LI-RADS major features at CT and MRI in 184 pathology proven hepatocellular carcinomas. *Abdom Radiol (NY)* 41:963–969
17. Corwin MT, Fananapazir G, Jin M, Lamba R, Bashir MR (2016) Differences in liver imaging and reporting data system categorisation between MRI and CT. *AJR Am J Roentgenol* 206: 307–312
18. Pickhardt PJ, Park SH, Hahn L, Lee SG, Bae KT, Yu ES (2012) Specificity of unenhanced CT for non-invasive diagnosis of hepatic steatosis: implications for the investigation of the natural history of incidental steatosis. *Eur Radiol* 22:1075–1082
19. Iannaccone R, Piacentini F, Murakami T et al (2007) Hepatocellular carcinoma in patients with nonalcoholic fatty liver disease: helical CT and MR imaging findings with clinical-pathologic comparison. *Radiology* 243:422–430
20. Fraum TJ, Tsai R, Rohe E et al (2017) Differentiation of hepatocellular carcinoma from other hepatic malignancies in patients at risk: diagnostic performance of the liver imaging reporting and data system version 2014. *Radiology* 286:158–172
21. Marrero JA, Hussain HK, Nghiem HV, Umar R, Fontana RJ, Lok AS (2005) Improving the prediction of hepatocellular carcinoma in cirrhotic patients with an arterially-enhancing liver mass. *Liver Transpl* 11:281–289
22. Grazioli L, Olivetti L, Fugazzola C et al (1999) The pseudocapsule in hepatocellular carcinoma: correlation between dynamic MR imaging and pathology. *Eur Radiol* 9:62–67
23. Bashir MR, Huang R, Mayes N et al (2015) Concordance of hypervascular liver nodule characterization between the organ procurement and transplant network and liver imaging reporting and data system classifications. *J Magn Reson Imaging* 42:305–314